Back Pressure Ratio and the Transonic Resonance Mechanism of Low Unchoking in Critical Flow Venturis

J. D. Wright[1], B. W. Sims[2], R. J. McKee[3], K. A. Gillis[1], A. N. Johnson[1], M. S. Carter[2], and Ida I. Shinder[1]

[1]National Institute of Standards and Technology, 100 Bureau Dr, Gaithersburg, MD, USA
[2]Flow Systems Inc., 220 Bunyan Ave, Berthoud, CO, USA
[3]Robert McKee Engineering LLC, Everett, WA, USA
E-mail (J. D. Wright): john.wright@nist.gov

Reliable Critical Flow Venturi (CFV) operation requires sonic velocity at the throat of the device. The maximum ratio of exit pressure to inlet pressure that ensures this sonic velocity is referred to as the maximum back pressure ratio (MBPR). Being able to accurately predict the MBPR for a specific CFV as well as design a CFV to have a high MBPR allows diverse application and confidence in CFV flow measurements. At Reynolds numbers based on throat diameter below 50 000, CFVs can display "low unchoking" and the standard equation over-reports the flow by 1 % or more.

We show that MBPR for a particular, 0.8 mm throat diameter CFV using dry air, argon, helium, and sulfur hexafluoride is well correlated by the "fully expanded jet Mach number". Sound detected by microphones placed up and downstream from a CFV show high correlation between low unchoking and the presence of powerful transonic resonances (oscillations at audio frequencies in pressure and the position of a lambda shock in the CFV diffuser) described by Zaman *et al.* We propose a mechanism in which pressure fluctuations from the transonic tones lead to intermittent unchoking of the CFV throat.

This paper also presents unchoking test results from 270 unchoking tests on 79 CFVs with a wide range of throat diameters, Reynolds numbers, diffuser lengths, half angles, and gases. Correlations for avoiding low unchoking and predicting MBPR for broader application are presented that incorporate the necessary effects due to *Re*, diffuser length, diffuser area ratio, and specific heat ratio. We advocate inclusion of these correlations in documentary standards.

1. Introduction

Critical nozzles are widely used as transfer standards to compare gas flow calibration capabilities or as working standards for calibrating other flow meters. Their advantages include stable calibration over long periods of time and a well understood physical model. Critical nozzles have the disadvantage of a large pressure drop relative to other gas flow meters, but this is improved by adding a diffuser for pressure recovery downstream from the throat. ISO and ASME [1, 2] standard designs for a critical flow venturi (CFV) use a conical diffuser with half angle θ between 2.5 and 6 degrees. Detailed drawings and definitions are provided in the standards. Using nomenclature defined at the end of this paper, the standard equation for mass flow is

$$\dot{m} = \frac{C_\mathrm{d} C_\mathrm{R}^* P_0 A^* \sqrt{M_\mathrm{m}}}{\sqrt{RT_0}}. \quad (1)$$

Equation 1 is only valid when the critical nozzle or CFV has small enough pressure ratio P_e/P_0 so that the gas velocity reaches the speed of sound at the throat, i.e. "choked" condition. The value of the discharge coefficient C_d is often based on a flow calibration against a reference standard, but can be calculated within 0.05 % from theory [3]. If the CFV is not choked, the standard mass flow equation will over-report the flow. The pressure ratio P_e/P_0 across the CFV that produces choked flow depends on the CFV geometry, Reynolds number, and the gas species. The largest P_e/P_0 value at which Equation 1 gives reliable flow values (within a specified tolerance) is called the maximum back pressure ratio (MBPR). The goals of this work are to (1) provide guidance on the MBPR necessary for choked flow for ISO/ASME standard CFV geometries and (2) develop better physical understanding of the relationship between the CFV shape and the MPBR.

Choked flow is a limiting condition where the fluid velocity reaches the speed of sound at the throat such that the mass flow will not increase with a further decrease in the downstream pressure [2]. In an unchoking test, a CFV is put in series with a flow reference (usually a second, smaller diameter CFV placed upstream) and the exit pressure P_e from the CFV under test is incrementally increased by closing a throttling valve until changes in the discharge coefficient of the CFV under test using Equation 1 are observed with respect to the reference flow meter [4]. When the change in C_d of the CFV under test is larger than a specified tolerance, the MBPR is noted and not exceeded during future operation.[1]

[1] The change in pressure upstream from the CFV under test could be used instead of the change in C_d that is normally plotted to indicate unchoking: when less of the throat area is at M = 1, the presure increases to maintain conservation of mass flow through the meters in series.

Compressible flow theory, assuming a calorically perfect gas (constant specific heats), one-dimensional (1-D), adiabatic, and inviscid flow predicts that the throat pressure ratio or MBPR necessary for choked flow without a diffuser is:

$$\left(\frac{P^*}{P_0}\right)_{\mathrm{crit}} = \left(\frac{2}{\gamma+1}\right)^{\gamma/(\gamma-1)}, \tag{2}$$

where γ is the specific heat ratio, c_P/c_V, P_0 is the stagnation pressure upstream from the critical flow venturi or nozzle, and $P^*$is the pressure at the CFV throat [5]. For dry air, $(P^*/P_0)_{\mathrm{crit}} = 0.53$, i.e. if the pressure at the throat is 53 % of the inlet pressure or less, the gas velocity will match the speed of sound at the throat, the CFV will be choked, and the flow is independent of the downstream pressure. Note that it is usually impractical to measure P^* in CFVs, especially when they have a small throat diameter. The exit pressure P_{e} is measured in the plenum downstream from the CFV diffuser exit and the pressure ratio P_{e}/P_0 is used instead of P^*/P_0 to assure a CFV is used in a choked condition.

The purpose of a CFV diffuser is to raise the pressure of the gas as it moves from the throat to the exit and thereby allow the CFV to be used for reliable flow measurement over a wider range of pressures. When the CFV diffuser is performing well, shock structures in the diffuser provide pressure recovery, P_{e} can be larger than P^*, and Equation 1 gives reliable flow values for a large range of P_{e}/P_0 values. MBPR > 0.95 is reported for some CFVs in air [6]. Research has shown that Equation 1 gives reliable flows for standard diffuser geometries for *Re* > 1×10^5 [6,7].

It is widely understood that the concept of choked flow and Equation 1 is an idealization and that in fact the flow is ***not*** sonic (*i.e.*, not at the speed of sound) across the entire area of the throat because of the boundary layer near the wall. Nonetheless, researchers [8, 9] were surprised to observe "low unchoking", i.e. that the flow through some CFVs departed significantly from Equation 1 at pressure ratios well ***below*** the values from Equation 2. An example is shown in Figure 1.

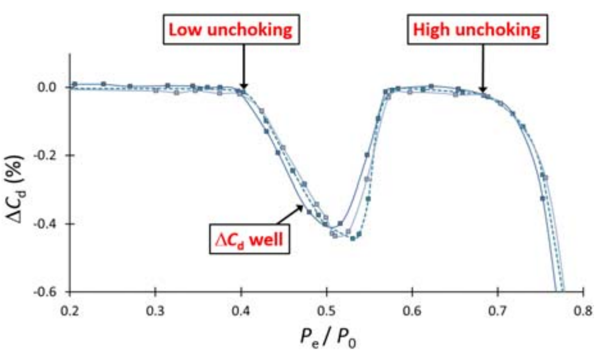

Figure 1. A plot of percent change in CFV discharge coefficient in air versus pressure ratio for CFV A14, *d* = 0.8 mm, diffuser length = 8.4 *d*, and θ = 2.5.

Figure 1 presents three sets of low unchoking data at nominally the same flow conditions for CFV "A14", a CFV that we will use as an example often in this paper. For air, the percent change in C_{d} should be zero for $P^*/P_0 < 0.53$, but for *Re* = 10080 (P_0 =100 kPa), there is a ΔC_{d} "well" as deep as 0.4 % for P^*/P_0 between 0.4 and 0.58.

Prior researchers of low unchoking have studied a variety of CFV designs that meet the ISO and ASME standards, testing various throat diameters, conical diffuser designs, pressure ratios, and gas species. Diffuser geometry is characterised by length and half-angle or exit to throat area ratio A_{e}/A^*.

Nearly every researcher of low unchoking has speculated that it is caused by the interaction of shocks in the diffuser with the boundary layer at the throat and diffuser entrance and possible flow separation. The "shock + boundary layer" explanation is supported by the absence of a ΔC_{d} well in quadrant nozzles. (A quadrant nozzle ends at the throat and has no diffuser.) The sharp edge at the exit of a quadrant nozzle establishes a centered Prandtl-Meyer expansion fan that thins the boundary layer. Consequently, quadrant nozzles have a thinner boundary layer than a CFV with a diffuser [10]. Moreover, the favourable pressure gradient from the Prandtl-Meyer expansion fan reduces the chance of boundary layer separation: a shock cannot occur until after the Prandtl-Meyer expansion fan, further downstream. The few CFVs with a step increase in diameter downstream from the throat that have been tested also do not show low unchoking presumably because of the consistent conditions at the intersection of the throat boundary layer and any shocks in the diffuser [7, 11].

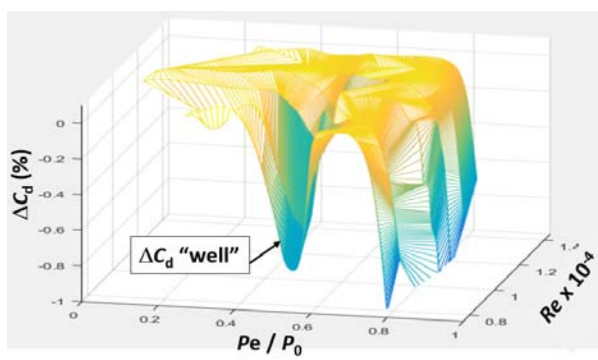

Figure 2. A surface plot of the change in discharge coefficient versus pressure ratio and Reynolds number for CFV A14 in air. At lower *Re*, the ΔC_{d} well is deeper, but the range of pressure ratios over which it occurs does not increase much.

For a given gas, low unchoking is also more prevalent and severe at lower Reynolds numbers, as shown in Figure 2. At low *Re*, momentum forces are small, the boundary layer in the throat and diffuser are significant portions of the cross sectional area and the diffuser is more prone to boundary layer separation. The boundary layer thickness in the diffuser affects the boundary layer thickness in the throat, as studied by Ding *et al.* [12]. For CFV A14 under the conditions that it was tested herein ($Re \cong 10{,}000$), the cross sectional area due to the boundary layer displacement thickness was approximately 3 % of the throat area.

Research by Carter *et al.* [7, 13] strived to better understand the source of low unchoking and established experimental guidelines for the MBPR that will give reliable CFV performance for particular diffuser geometries. They have coined the term “diffuser performance inversion” instead of the original term “premature unchoking” to highlight that low unchoking is related to the performance of the diffuser and that a CFV is always unchoked to some degree due to the presence of a subsonic boundary layer. Part of the objection to the term premature unchoking is that it seems likely that there is still a portion of the throat that is moving at $M = 1$, at least some of the time. In this paper, we use the terms low unchoking and high unchoking (Figure 1).

It should be emphasized that the ΔC_{d} due to low unchoking is only significant at the 0.01 % level for Reynolds numbers below 1×10^5. This may occur when using CFVs smaller than 2 mm. Furthermore, even CFVs much smaller than 2 mm are reliable flow sensors if plots like Figures 1 or 2 are available and followed. Also, empirical studies of standardized geometries (which show that long diffusers are less susceptible to low unchoking) are a practical approach.

2. Proposed mechanism for low unchoking: transonic resonance

The shock structures of conical diffusers have been visualized and studied extensively by prior researchers. The shocks depend on the geometry of the diffuser (half angle, length, surface roughness), the gas specific heat ratio, the Reynolds number (and the boundary layer thickness), and whether the boundary layer is laminar or turbulent. A review of the prior literature reveals a progression of shock conditions as P_{e}/P_0 varies that we depict in Figure 3.

Figure 3a illustrates the CFV at low pressure ratios. The flow expands via a Prandtl-Meyer fan that originates at the change in curvature between the toroidal and conical sections of the diffuser. A plot of the pressure versus streamwise location is also shown at the bottom of Figure 3a. The favourable pressure gradient downstream of the throat leads to a thinning of the boundary layer and helps keep it attached to the diffuser wall.

Figure 3b illustrates an oscillating shock within the diffuser that generates what Zaman *et al.* [14] call “transonic resonance”. Zaman and Papamoschou *et al.* [15] demonstrated that a lambda shock (a combination of a normal and an oblique shock) forms in the diffuser over a range of pressure ratios and that the shock oscillates in a piston-like manner. Papamoschou *et al*. measured shock oscillations in a 2-D diffuser via the coherence of high-frequency pressure measurements made at taps on opposite sides of the diffuser. Zaman *et al.* measured peaks in the acoustic spectra from a microphone placed downstream from CFVs with various diffuser geometries. Zaman *et al.* referred to these peaks as “transonic tones” or “x-tones”. The existence of transonic tones correlates with researchers noting an audible change in the sound emanating from a CFV depending upon whether it is choked are not [16]. Transonic resonance occurs only when the shock is within the diffuser. External shocks cause screech tones at low pressure ratios [14].

The time-averaged position of the lambda shock moves upstream (closer to the throat) as P_{e}/P_0 is increased. The pressure rise across the lambda shock produces a strong, oscillating adverse pressure gradient that triggers boundary layer separation. The oscillating lambda shock causes periodic changes in the boundary layer thickness and periodic flow separations. We hypothesize that when the pressure oscillations from the lambda shock resonances are sufficiently powerful and close to the CFV throat (or P_{e}/P_0 is sufficiently high), the sonic core flow is disturbed in a periodic manner as well, causing low unchoking, as depicted in Figure 3c.

This explanation agrees with von Lavante’s [17] observation from a computational fluid dynamic simulation of a CFV: “At approximately, [P_{e}/P_0] = 0.4, it displays a clear sign of low unchoking, again, due to unsteady movement of the lambda shock upstream all the way through the throat.”

The nature of the disturbance of the sonic core by transonic resonance is not known, but we propose two possible mechanisms: 1) the sonic core is periodically changing in size due to periodically thickening boundary layer and separation in the diffuser and 2) the drum-like motion of the lambda shock within the diffuser in the axial direction produces periodic pressure oscillations immediately downstream from the throat that lead to movement and area changes of the sonic core and/or the sonic core choking and unchoking in a periodic manner.

Figure 3d depicts the situation at higher pressure ratios where the shocks are non-existent or so weak, symmetric, and stable that they no longer cause flow separation near the throat. The lack of a strong shock within the diffuser means that the adverse pressure gradient is weak and separation is less likely. For these conditions, the sonic core is stable at the geometric throat position and ΔC_{d} returns to near zero.

In section 4, we will present acoustic spectra along with low unchoking test data that show strong correlation between the transonic tones and low unchoking.

Accurately predicting the location, period, and pressure rise of the shocks depicted in Figures 3b and 3c and the occurrence of separation is a yet unsolved topic of research. Therefore, it is presently impractical to predict the onset of low unchoking for a given CFV, gas species, and pressure condition. However, in later sections, we assemble experimental results to guide users regarding what pressure ratios are required for reliable flow measurements from standard CFV designs.

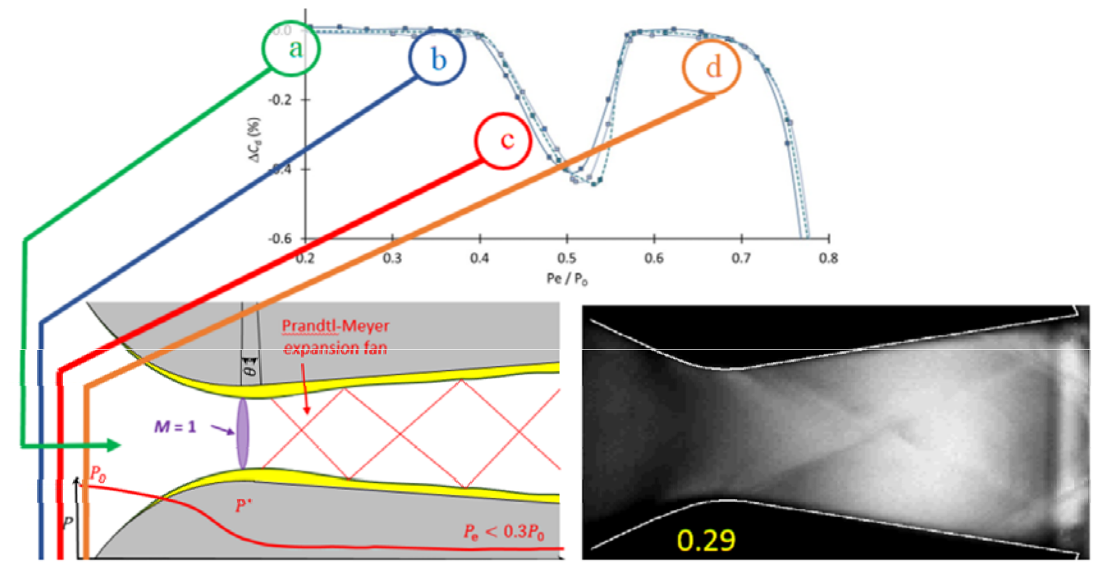

a) Prandtl-Meyer expansion fan causing favorable pressure gradient in diffuser, attached boundary layer near throat, stable sonic core at geometric throat. Various shock structures may be present at the diffuser outlet (under, perfectly, or over expanded).

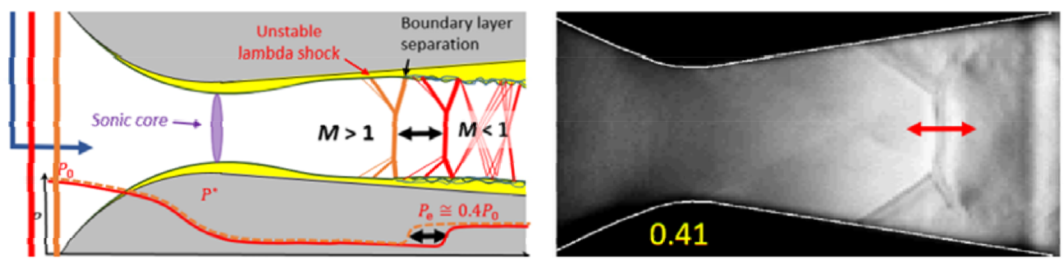

b) Transonic resonance, oscillating lambda shock, strong adverse pressure gradient at shock, boundary layers separated, stable sonic core at the geometric throat.

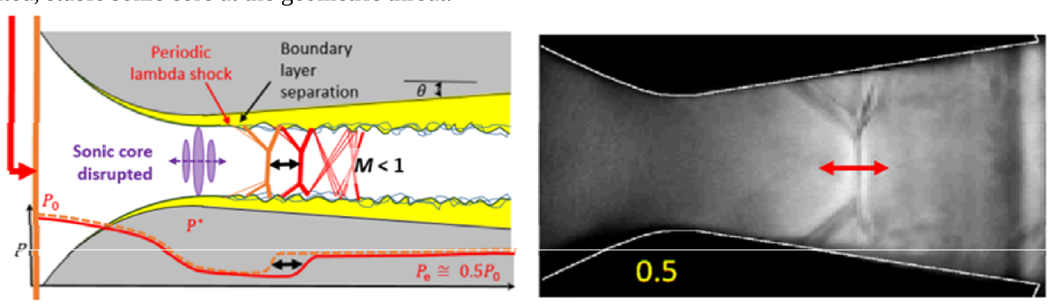

c) Transonic resonance, oscillating lambda shock, strong adverse pressure gradient at shock, boundary layers separated, disrupted sonic core.

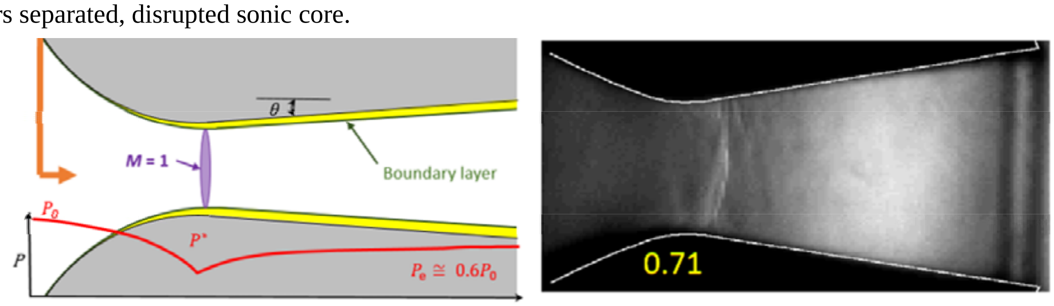

d) CFV just choked, no strong shocks, weak adverse pressure gradient in the diffuser, boundary layers attached, stable sonic core at the geometric throat.

Figure 3. Left) Schematic shock structure and boundary layer interactions and their role in low unchoking. **Right)** Schlieren photograp hs of a 2-D CFV from Hunter [18], labelled with their P_e/P_0 values. Note that the dark vertical lines at the CFV exit are apparently not shocks: they are present in all of the images.

3. Characteristics of transonic tones

In this section, we review the work of Hunter [18], Zaman [14], and Papamoschou [15] and their many colleagues to better understand the flow phenomena in a nozzle diffuser and the characteristics of transonic resonances.

Zaman states that transonic resonances are longitudinal acoustic modes of the diffuser that are modified by the flow. The conical diffuser forms a ¼ wave resonator with modes that have an acoustic pressure antinode at the position of the lambda shock and a node near the diffuser exit. Thus, the lowest-frequency (fundamental) resonance occurs when the wavelength of sound is about 4 times the distance between the shock and the diffuser exit: higher-frequency resonances occur at odd multiples of the fundamental. Zaman compares the lambda shock to the head of a drum. He said the resonance amplitude "is not well defined and sensitive to e. g. the surface finish." When the lambda shock is in the diffuser (Figures 3b and 3c), as P_e/P_0 increases, the distance between the lambda shock and the diffuser exit increases (the shock moves towards the throat), thereby the resonance wavelength increases and the frequency decreases. This behaviour is the opposite of screech tones which increase in frequency with increasing P_e/P_0.

Zaman presented correlations that allow prediction of the transonic resonance frequency as a function of the diffuser length, half angle, the speed of sound, and the fully expanded jet Mach number, M_j defined by

$$M_j \equiv \left[\left[\left(\frac{P_0}{P_e}\right)^{\frac{\gamma-1}{\gamma}} - 1\right]\frac{2}{\gamma-1}\right]^{1/2} . \qquad (3)$$

M_j is the Mach number that would be present at the exit of the diffuser for an adiabatic, isentropic, and inviscid flow (no boundary layer and no shocks), for a perfect gas, with constant specific heats. Zaman's correlation worked well for diverse geometries, axisymmetric, 2-D, and annular, i.e., similar transonic phenomena occur in various CFV geometries.

Both Zaman and Papamoschou found the lambda shock at much smaller area ratios A/A^* than predicted by 1-D theory, i.e. closer to the throat.

Figure 4a shows Hunter's centerline pressure data for a range of P_e/P_0's, labelled with the corresponding schematics from Figure 3. Successful diffuser performance and pressure recovery, without sonic core disruption occur at high P_e/P_0's (labelled Fig. 3d). Intermediate pressure ratios that show low unchoking in CFV A14 have large, oscillating pressure gradients near the throat (Fig. 3c). For the lower pressure ratios labelled Fig. 3b and 3a, the shocks are near the exit, and low unchoking is not present (at least for CFV A14).

Papamoschou [15] found that the oscillating lambda shock "creates a 'back pressure' much higher than the theory predicts" for a stationary shock. Figure 4b shows the pressure measured with a probe on the centerline, deconvoluted to remove lags from the sensor's time constant, to give a better idea of the real pressure fluctuations.

Zaman found that the transonic resonance only occurred when the nozzle surface was smooth and that the tones disappeared if the boundary layer was tripped by small protrusions or pieces of tape upstream of the lambda shock location. This suggests that a CFV with a stepped diffuser, *i.e.* a small step increase in the diffuser diameter, would not have transonic tones.

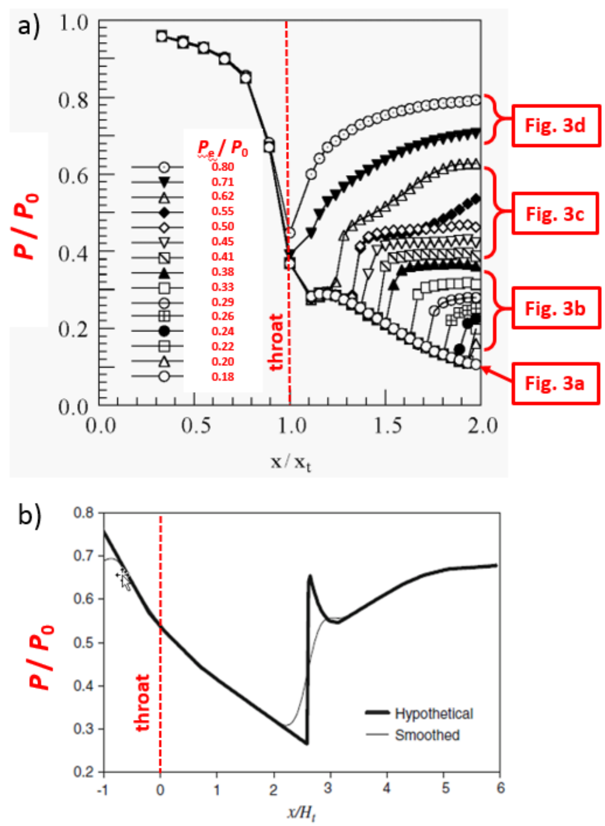

Figure 4. Centerline pressure in 2-D diffusers, with our annotations in red font. **a)** from Hunter [18] for *Re* = 3.2 × 10[6], H_t = 14 mm, L = 53.8 mm, θ = 11°, and **b)** from Papamoschou [15], showing underestimation of pressure changes due to sensor time response for a trumpet shaped diffuser at *Re* = 2.1 × 10[5], L = 117 mm.

4. Acoustic spectra for CFV A14

We installed two microphones, one upstream and one downstream from CFV A14. The CFV was installed with 2.2 cm approach and exit tubes and the microphones were installed via 1.0 cm inside diameter Tees (Figure 5). Using a spectrum analyser, we measured the acoustic frequency spectrum that was present for various pressure ratios traversing the low unchoking phenomenon in dry air. Strong acoustic resonances and their harmonics were detected at pressure ratios correlated with low unchoking.

Using the manufacturer specified diffuser length and half angle, the frequencies of the resonances were 2 % to 13 % lower than those predicted by Zaman's correlation (Table 2).

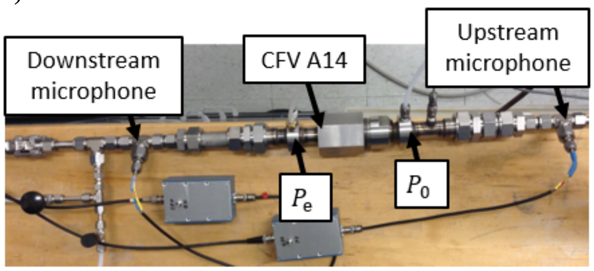

Figure 5. Positions of CFV A14, pressure sensors and microphones for acoustic spectra.

Figure 6 shows spectra from the downstream microphone for P_e/P_0 ranging from 0.3 to 0.6. The fundamental frequency was nominally 14 kHz and the 2nd and 3rd harmonics are also visible in Figure 6a at ≅ 28 kHz and ≅ 42 kHz. For the fundamental mode, resonance peaks > 100 Pa^2 were present for pressure ratios between 0.35 and 0.57. Figure 6b zooms in on the fundamental mode outlined by the dashed box and uses a linear scale to make their relative power more apparent.

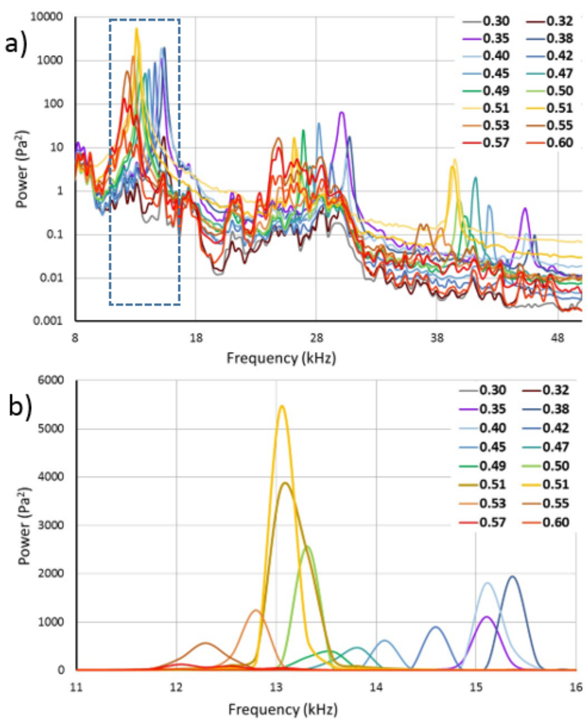

Figure 6. Acoustic spectra from the downstream microphone for various pressure ratios.

Figure 7 shows spectra from the upstream microphone. The resonance peaks are weaker and are present over a narrower and higher range of pressure ratios.

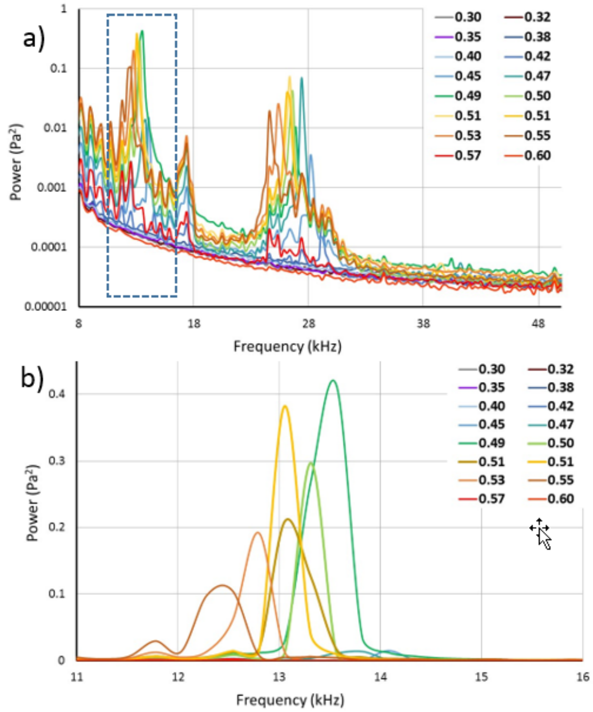

Figure 7. Acoustic spectra from the upstream microphone.

Figure 8a shows the frequency of the fundamental transonic tones versus P_e/P_0 for both the up and downstream microphones, along with the ΔC_d data gathered in unchoking measurements conducted at the same time. Data from two experiments are presented to assess reproducibility. The upstream and downstream frequencies match, as shown in Figure 8a. The frequency of the tones decreases with increasing pressure, matching the behaviour of transonic resonance described by Zaman (as opposed to screech tones).

Figure 8b plots the acoustic power versus P_e/P_0 for the two sets of data in air. The largest values of acoustic power from the downstream and upstream microphones and the minimum of the ΔC_d well coincide at $P_e/P_0 \cong 0.5$. The transonic tones are not detected on the upstream side of the CFV until $P_e/P_0 = 0.45$, well into the ΔC_d well and their power is approximately three orders of magnitude lower than on the downstream side. There are strong transonic tones downstream at $P_e/P_0 = 0.38$ where $\Delta C_d = 0$, while at $P_e/P_0 = 0.45$ the power from the downstream microphone is relatively low, but unchoking is significant.

Based on a simple model (the ratio of cross sectional area at the pipe where the downstream microphone was installed to the area of the throat), we estimate the acoustic pressure fluctuations to be 170 times stronger at the CFV throat than at the microphone, or as much as 13 kPa on the downstream side.

A possible explanation for the data in Figure 8a is that for low unchoking to occur, the oscillating pressure component downstream from the throat must be sufficiently large to cause the throat to be intermittently sonic or subsonic, as illustrated in Figure 9.

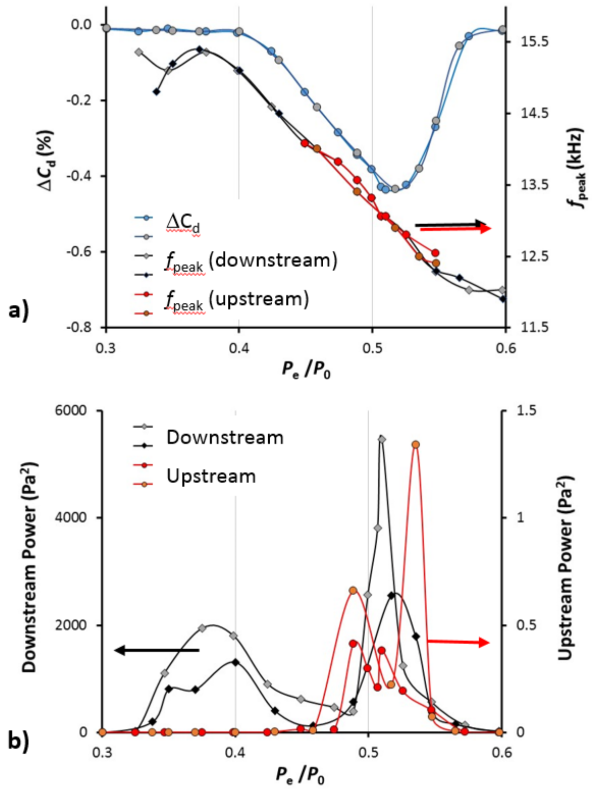

Figure 8. a) ΔC_{d}, resonant frequencies, and **b)** acoustic power from the two microphones, versus pressure ratio.

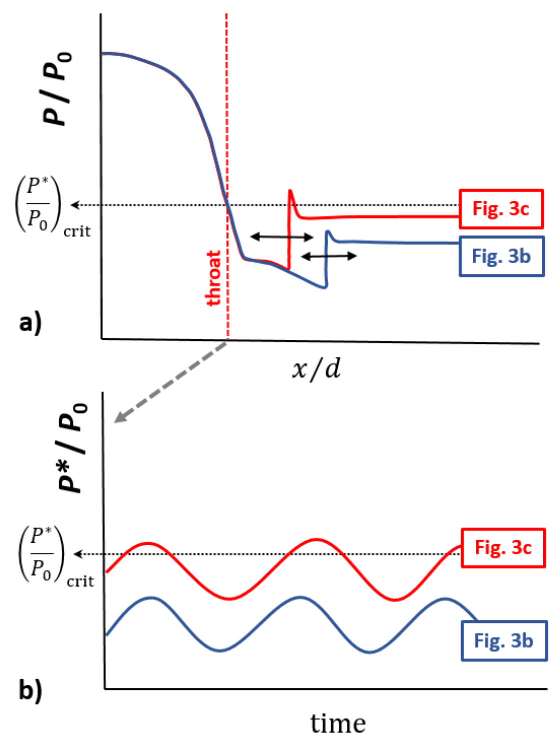

Figure 9. Illustration of how transonic pressure fluctuations could cause an intermittent sonic core because pressure ratio at the throat periodically exceeds $(P^*/P_0)_{\text{crit}}$, **a)** plotted versus position and **b)** at the throat versus time.

5. Low unchoking of CFV A14 for gases with various specific heat ratios

Many aspects of the flow through a CFV depend on the gas specific heat ratio, γ, for instance, the angle of oblique shocks and the pressure rise across a normal shock. The fully expanded jet Mach number M_{j} used to characterize the transonic tones is also a function of γ. Figure 10a shows ΔC_{d} versus P_{e}/P_0 for CFV A14 using sulfur hexafluoride, dry air, helium, and argon.

In this experiment, we designed the test conditions to provide the same boundary layer thickness at the CFV throat for all of four gases to see if the low unchoking plots would match. CFD simulations of a CFV performed by Johnson [19] show that the boundary layer thickness depends on both Re and γ. (The specific heat ratio affects the temperature in the boundary layer and larger γ causes a thicker boundary layer.) Based on Figure 3.12 in reference [19], we performed the unchoking tests at the Reynolds numbers (or P_0 values) listed in Table 1, appropriate to achieve a displacement thickness that comprised 3 % of the throat area for each gas.

Table 1. Test conditions to produce same displacement thickness in d = 0.8 mm CFV A14 for various gases.

Gas	γ [-]	Re [-]	P_0 [kPa]
SF_6	1.10	9400	37.6
Dry air	1.40	10080	100.5
Ar	1.67	10500	104.9
He	1.67	10500	287.1

Figure 10a shows the results from eight low unchoking tests for the four gases plotted versus P_{e}/P_0 (same air data as Figure 1) and Figure 10b uses the inverse of the Mach jet number as the abscissa. The onset of low unchoking is better correlated by the jet Mach number than by P_{e}/P_0. Differences in the depth of the ΔC_{d} wells remain in both plots (0.19 %), despite controlling for equal boundary layer thicknesses across the four gases. In another experiment where all four gases were tested at the same Reynolds numbers (not shown here), the depths of the ΔC_{d} wells varied by 0.32 %, supporting the idea that the boundary layer thickness (not Reynolds number alone) is important in the low unchoking phenomenon. The two gases with the same specific heat ratios (helium and argon) show nearly the same low unchoking behaviour. We note that the bottom of the ΔC_{d} wells is at $M_{\mathrm{j}} \cong 1$, which corresponds to the critical back pressure given by Equation 2 for each gas.

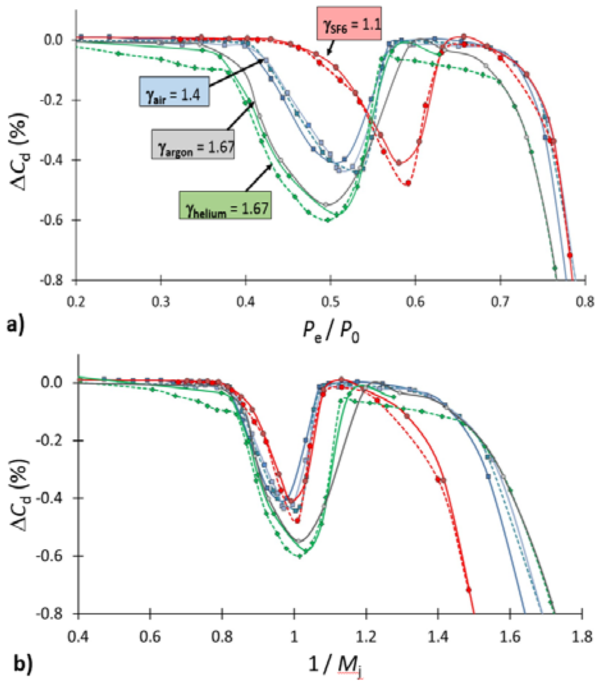

Figure 10. Change in discharge coefficient versus **a)** pressure ratio and **b)** inverse jet Mach number, for various gases in CFV A14.

Acoustic spectra were also gathered for A14 flowing sulfur hexafluoride and helium. The spectra were qualitatively similar to those presented herein for air, but the frequency of the tones was quite different. The frequency of the transonic resonances, measured and predicted using Zaman's correlation are listed in Table 2.

Table 2. Resonant tone frequency at bottom of ΔC_d well, measured and calculated following Zaman [14].

Gas	Measured f_{peak} [kHz]	Calculated f_{peak} [kHz]
SF_6	5.38	5.25
Dry air	13.1	11.6
He	34.8	30.4

6. Avoiding low unchoking

We have learned much about the mechanism of low unchoking and can make reasonable predictions of the frequency of transonic tones, but not their power. So, theoretically predicting the onset of low unchoking for an arbitrary geometry is not yet practical. Several practical approaches are available for designing CFVs that do not or are less likely to exhibit low unchoking:

1) Reduce the diffuser length to 1*d*, per ISO 9300 and ASME MFC-7, and operate these CFVs at back pressures below the critical pressure given by Equation 2,

2) Add a diffuser step just downstream of the CFV throat to ensure stability of the shock structure,

3) Extend the diffuser length to 15*d* or more to provide a sufficiently low pressure gradient to suppress low unchoking per proven performance of similar CFVs,

4) Use the correlation equation given below, generated from unchoking data to design a CFV that will not demonstrate low unchoking at the minimum operational Reynold Number.

1) Reduction of the CFV diffuser length to 1*d*, the minimum length allowable by the ISO and ASME [1, 2] CFV standards, has been shown, in the vast majority of tested cases, to eliminate low unchoking. A 1.575 mm CFV with a $\theta = 4°$ and a 5.3*d* long diffuser demonstrated low unchoking when tested. The diffuser was then shortened to 1*d* and re-tested at a similar Reynolds number, and no low unchoking was observed, as shown in Figure 11. The disadvantage of using this method to avoid low unchoking is the loss of pressure recovery in the diffuser resulting in a much lower maximum back pressure ratio than could be attained with a longer diffuser.

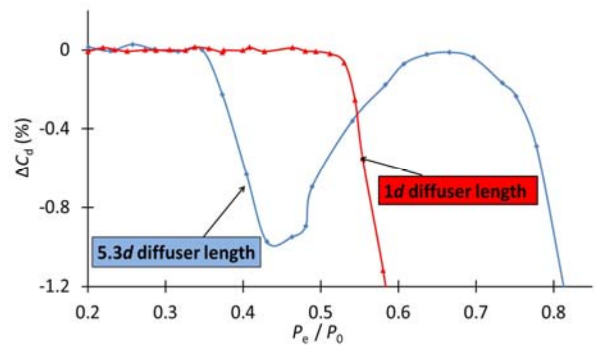

Figure 11. Elimination of low unchoking with 1*d* diffuser length.

2) An increasing diameter "step" in the diffuser has been shown to prevent low unchoking. Two CFVs of similar geometry, except one with a diffuser step, were tested and the results can be seen in Figure 12. The work of Xu *et al.* [20] shows that "crest structures" as small as 2 nm near the throat cause large differences in low unchoking behaviour in a *d* = 200 µm CFV. We conclude that in small CFVs, the boundary layer trip should be a step of increasing diameter, not a raised surface. The step should be located approximately 1*d* from the throat of the CFV and result in a diffuser cross-sectional area increase of about 1%.

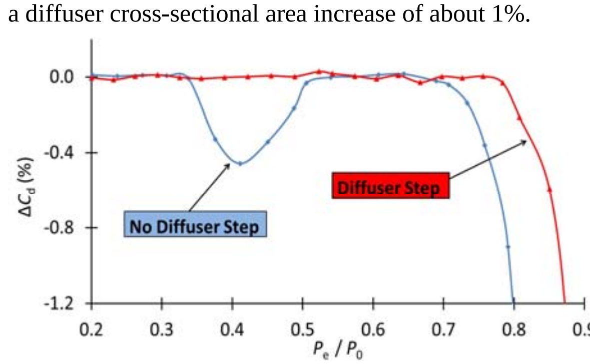

Figure 12. Elimination of low unchoking with a diffuser step.

3) Data from a range of small CFVs with 10*d* and 15*d* diffusers show that for the longer diffusers, low unchoking was not observed for *Re* > 3000 [11]. Such long diffusers reduce the pressure gradients in the flow where the shock

structure occurs and thereby avoid the occurrence of low unchoking.

4) Data from 270 unchoking tests on 79 CFVs with throat diameters from 0.39 mm to 12.7 mm, Re = 2800 to 240 000, $\theta = 2.5$ to 6 degrees, $L = 4.9d$ to $20d$, and $\gamma = 1.09$ to 1.67 were studied regarding the occurrence of low unchoking (Figure 13). Throat diameters were corrected from the assumed values to match the C_{d} equation provided by the ISO Standard [1] to reduce error in Reynolds numbers. Diffuser length and Reynolds number were found to be the most significant factors correlated to the occurrence of low unchoking. While some data show magnitude and back pressure location variations in low unchoking due to the specific heat ratio, no significant correlation between occurrence and lack of occurrence was found. The apparent sensitivity of low unchoking to surface finish and imperfections (which was not measured) probably lead to some scatter in the results. To avoid low unchoking it is recommended that diffuser length, L (in throat diameters) should conform to

$L/d \geq \max(5.0, 11.89 - 1.556 \times 10^{-4} Re)$,(4)

valid for $Re > 2800$, $1.09 < \gamma < 1.67$, and $2.5° < \theta < 6°$.

Equation 4 is designed to take into account expected surface finish variations from manufacturing. It is conservative, correctly avoiding 100 % of occurrences of low unchoking in the test data. This is shown in Figure 13 as all low unchoking events occur to the left of the red line. The equation provides recommended diffuser length for a specified minimum operation Reynolds number.

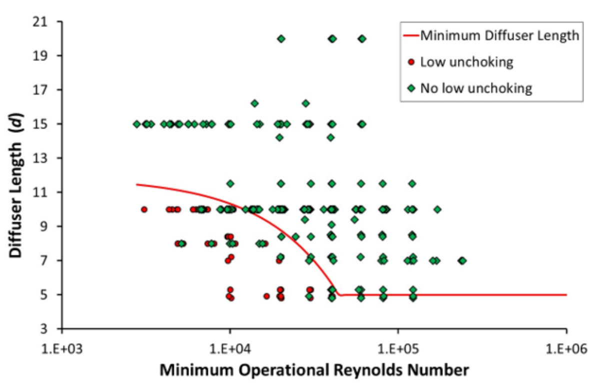

Figure 13. Diffuser length versus Reynolds number plot for avoidance of low unchoking.

7. Correlation Equation for predicting MBPR

Using the data from all the unchoking tests that didn't display low unchoking, a correlation equation for predicting maximum back pressure ratio was developed. MBPR was found to be influenced most strongly by Reynolds number but was also sensitive to throat diameter, diffuser length, and diffuser half angle. The correlation equation was designed to be conservative, predicting MBPR values that are equal to or lower than 95% of the collected data.

$$MBPR = 1.0305 - \frac{19.49}{{R_e}^{0.5}} + 3.247 \times 10^{-2} \ln\left(\frac{d}{25.4}\right) - 3.316 \times 10^{-2}\theta + 2.354 \times 10^{-3}\frac{L}{d}, \quad (5)$$

where d is in mm. Equation 5 is valid for $2800 < Re < 240\,000$, $1.09 < \gamma < 1.67$, $2.5° < \theta < 6°$, and $L/d > 5$.

Table 3. Example values for MBPR correlation equation.

d [mm]	L/d [-]	θ [°]	Re [-]	MBPR [-]
0.41	11	3	6835	0.59
0.56	11	4	9455	0.60
0.79	10	4	13395	0.64
1.12	9	5	19100	0.64
1.60	8	5	27456	0.68

8. Summary and conclusions

We have shown strong correlation between low unchoking and the presence of a transonic resonance described by Zaman [14], Papamoschou [15], and others. We propose that low unchoking is due to interactions of the transonic resonance with the boundary layer *and* the sonic core at the throat (Figure 3c). This explanation matches the ideas of prior experimental and computational researchers and accounts of audible tones during low unchoking.

The mechanisms for low unchoking and transonic resonance are interactions between acoustics and fluid mechanics that are still incompletely understood. But a complete physical model will likely include: 1) acoustic modes of a cone, 2) oscillatory pressures due to movement of the lambda shock in the diffuser, and 3) the boundary layer thickness in the throat and separation in the diffuser. Flow separation occurs downstream from lambda shocks and may trigger the shock oscillations.

Low unchoking is strongly dependent on the Reynolds number, establishing that a thick boundary layer is a prerequisite to the problem. In this study we found that the depth of the ΔC_{d} wells better matches across various gas species when boundary layer thicknesses are matched rather than just Re. We also found that the jet Mach number correlates the onset of low unchoking across gases with different specific heat ratios (Figure 10b).

We project from our new understanding of transonic resonance in CFVs and some experimental evidence (Figure 12) that there is a practical remedy for low unchoking: a “stepped diffuser”, i.e., a diffuser with a small step increase in diameter near the geometric throat. Zaman states, “The resonance ceases when the shock location has moved sufficiently downstream when the flow can no longer support the ¼ wave” [14]. A step 1) reduces the boundary layer thickness (see Ding *et al.* [12]), 2) trips the boundary layer from laminar to turbulent (helping it remain attached like the dimples on a golf ball) and 3) anchors a Prandtl-Meyer expansion fan and forces normal shocks further downstream, away from the throat. We plan to perform more experiments with stepped diffusers to check that they eliminate low unchoking for various diffuser geometries and still deliver the desired pressure recovery. We also want to study the nature of the higher harmonics of the transonic resonance and why the jet Mach number collapses low unchoking results for different gas species.

Finally, we presented practical correlations that allow CFV users to avoid low unchoking for CFVs that meet the ISO and ASME standard geometries and recommend that ISO and ASME include the correlations in future CFV standards.

9. Acknowlegements

This work was partially sponsored by the US Department of Defense Calibration Coordiantion Group, Physical / Mechanical Project # 654. We also thank Iosif Shinder and our NIST SURF student, Sam McClung for Figure 2.

Nomenclature

$A^* = \pi d^2/4$	CFV throat area at reference temperature
A_e	CFV diffuser exit area
$C_\mathrm{d} = \dot{m}_\mathrm{ref}/\dot{m}_\mathrm{CFV}$	Experimental CFV discharge coefficient
c_P	Constant pressure specific heat
c_V	Constant volume specific heat
C_R^*	Real gas critical flow factor (calculated from a thermodynamic database [21])
d	CFV throat diameter
f_peak	Frequency of the highest amplitude sound in acoustic spectrum
H_t	Height of throat in a 2-D nozzle
L	Diffuser length
MBPR	Maximum back pressure ratio
M_m	Gas molar mass
M	Mach number
$\dot{m}_\mathrm{ref}$	Mass flow measured with a reference flow standard
$\dot{m}_\mathrm{CFV}$	Mass flow through a CFV calculated by theoretical or analytical means
P^*	Stagnation pressure at the CFV throat
P_0	Stagnation pressure at the CFV inlet
P_e	Stagnation pressure at the CFV exit
$Re = \dfrac{4\dot{m}}{\pi d \mu_0}$	Reynolds number, using the throat diameter as length scale, μ_0 is the dynamic viscosity based on P_0 and T_0
R	Universal gas constant
T_0	Stagnation temperature in the CFV approach pipe
γ	Ratio of constant pressure and constant volume specific heats, $= c_P/c_V$
θ	CFV diffuser half-angle

[1] International Standards Organization, *Measurement of Gas Flow by Means of Critical Flow Venturi Nozzles*, ISO 9300, 1st edition,1990, 2nd edition, 2005.

[2] American Society of Mechanical Engineers, *Measurement of Gas Flow by Means of Critical Flow Venturis and Critical Flow Nozzles*, ASME MFC-7-2016.

[3] Johnson, A. N. and Wright, J. D., *Comparison between Theoretical CFV Models and NIST's Primary Flow Data in the Laminar, Turbulent, and Transition Flow Regimes*, ASME Journal of Fluids Engineering, vol. 130, July, 2008.

[4] Nakao, S.-I. and Takamoto, M., *Choking Phenomena of Sonic Nozzles at Low Reynolds Numbers*, Flow Meas. Instrum., 11, pp. 285 to 292, 2000.

[5] Anderson, J. D., *Modern Compressible Flow*, 3rd ed., McGraw Hill, 2004.

[6] Hillbrath, H. S., Dill, W. P., and Wacker, W. A., *The Choking Pressure Ratio of a Critical Flow Venturi*, J. Eng. Ind., Ser. B, **97**, no. 4, pp. 1251 to 1256, 1975.

[7] Carter, M. S., Sims, B. W., and McKee, R. J., *Choking Pressure Ratio Guidelines for Critical Flow Venturis and the Study of Diffuser Pressure Distribution*, Proceedings of the 9th International Symposium on Fluid Flow Measurement, Arlington, Va, USA, April 14 to 17, 2015.

[8] Britton, C. L. and Caron, R. W., *Unchoking Pressure Ratio for Critical Flow Venturis*, FEDSM97-3004, Proceedings of the ASME Fluids Engineering Summer Meeting, Vancouver, Canada, 1997.

[9] Ishibashi, M., *Study of the Standard of Gas Flow Rate Using Sonic Nozzles and Its Application Techniques*, NRLM Tsukuba, 1996.

[10] Ishibashi, M. and Takamoto, M., *Methods to Calibrate a Sonic Nozzle and Flowmeter Using Reference Critical Nozzles*, Flow Meas. Instrum., 11, pp. 293 – 304, 2000.

[11] von Lavante, E., Zachcial, A., Zeitz, D., Dietrich, H., and Nath, B., *Effects of Various Geometric Parameters on Flow Behavior in Sonic Nozzles*, Proceedings of FLOMEKO, Salvador, Brazil, Paper F6, 2000.

[12] Ding, H., Wang, C., Zhao, Y., *Influence of Divergent Section on Flow Fields and Discharge Coefficient of ISO 9300 Toroidal-Throat Sonic Nozzle*, Flow Meas. Instrum., 40, pp. 19 to 27, 2014.

[13] Carter, M. S., Sims, B. W., Britton, C. L. and McKee, R. J., *Choking Pressure Ratio Guidelines for Small Critical Flow Venturis and the Effects of Diffuser Geometry*, Proceedings of FLOMEKO, Paris, France, Paper B3.4, 2013.

[14] Zaman, K. B. M. Q., Dahl, M. D., Bencic, T. J. and Loh, C. Y., Investigation of a 'Transonic Resonance' with Convergent-Divergent Nozzles, J. Fluid Mech., **463**, pp. 313 to 343, 2002.

[15] Papamoschou, D., Zill, A., and Johnson, A., *Supersonic Flow Separation in Planar Nozzles*, Shock Waves, 19, 171, July 2009.

[16] Ishibashi, M., *Super-Fine Structure in the Critical Flow-Rate of Critical Flow Venturi Nozzles*, FEDSM2002-

31079, Joint US-European Fluids Engineering Conference, Montreal, Canada, 2002.
[17] von Lavante, E., Winzosch, F. and Brinkhorst, S., *Detailed Study of Flow Structure in CFVN and its Effects on the Flow Rate*, Proceedings of FLOMEKO, Paris, France, Paper A3.5, 2013.
[18] Hunter, C. A., *Experimental, Theoretical, and Computational Investigation of Separated Nozzle Flows*, 34th AIAA/ASME/SAE/ASEE Joint Propulsion Conference and Exhibit, Cleveland, Ohio, USA, July 13 to 15, 1998.
[19] Johnson, A. N., *Numerical Characterization of the Discharge Coefficient in Critical Nozzles*, Ph.D. Thesis, Pennsylvania State Univ., University Park, Pennsylvania, USA, 2000.
[20] Xu, M., Kauth, F., Mickan, B., and Brand, U., Traceable Profile and Roughness Measurements Inside Micro Sonic Nozzles with the Profilscanner, 17th International Congress of Metrology, 13004, 2015, http://dx.doi.org/10.1051/metrology/20150013004.
[21] Lemmon E. W., Huber M. L., and McLinden M. O., *NIST Standard Reference Database 23: Reference Fluid Thermodynamic and Transport Properties-REFPROP*, Version 9.0 National Institute of Standards and Technology, Standard Reference Data Program, Gaithersburg, 2007.